An Overview of the MRI/JMA 20-km Mesh Atmospheric General Circulation Model and a Global Warming Time-Slice Experiment

Akio KITOH[1], Akira NODA[2], Shoji KUSUNOKI[3] and Kyosei4-sub1 members

Meteorological Research Institute (MRI),

1-1 Nagamine, Tsukuba, Ibaraki 305-0052, JAPAN

e-mail: [1]kitoh@mri-jma.go.jp, [2]noda@mri-jma.go.jp, [3]skusunok@mri-jma.go.jp

1. Model and experiment

We present future climate change projections over Turkey and the East Mediterranean region conducted by a time-slice experiment with a super-high resolution atmospheric general circulation model (20-km mesh TL959L60 MRI/JMA AGCM) performed by the RR2002 project "Development of Super High Resolution Global and Regional Climate Models"(Aoki et al. 2004).

The global model framework is designed to become a next generation numerical weather prediction model of the Japan Meteorological Agency in this resolution (global 20-km mesh). A lower resolution version will be used as an atmospheric part of the third generation atmosphere-ocean coupled general circulation model of MRI. The model is a spectral model with wave number 959 in a linear grid with 1920 x 960 grid points. Semi-Lagrangian two time-level scheme is developed, which enabled us an efficient time integration. A one-year integration of TL959L60 model takes about 50 hours wall clock time using 30 nodes (240 processors) of the Earth Simulator.

First, a 10-year control simulation was done with the climatological observed sea surface temperature (SST) corresponding to the 1982-1999 period. Next, another 10-year global warming simulation (time-slice experiment) was performed by adding the SST anomalies derived from the MRI-CGCM2.3 (Yukimoto et al. 2001; T42L30 atmosphere, 0.5-2.0 x 2.5 L23 ocean) SRES A1B scenario experiment corresponding to the end of the 21st century (2081-2100 mean).

2. Results

Figure 1 shows the seasonal mean precipitation in the history run corresponding to the present climate. Validation of model climatology with respect to mean and variability will be performed in a different report, but the seasonal cycle in precipitation, temperature and circulation fields is well reproduced in the model.

There is a seasonal difference in the magnitude of surface air temperature changes over Turkey (figures not shown). A large increase in surface air temperature of about 3°C is projected over Turkey in summer, while it is between 1°C and 2°C in winter. Larger rise in temperature in summer in the subtropical land areas is noted in IPCC (2001).

Figure 2 shows the changes in seasonal mean precipitation at the end of the 21st century simulated by the MRI/JMA TL959L60 AGCM. Large decrease in precipitation is found in winter (DJF) around the southern coastal region of Turkey, particularly over the eastern Mediterranean Sea. It is noted that an area of large precipitation decrease is extended into the lower Seyhan River Basin, which is the ICCAP project target region, blocked by the Toros mountains to the north. There is an increase in precipitation over the northern coastal region in Turkey facing the Black Sea. Situation changes in spring (MAM), when magnitude in precipitation changes over the Mediterranean Sea becomes smaller, and even a sign of precipitation changes becomes opposite from that in winter in some areas, in particular over the ICCAP region of the lower Seyhan River Basin. Central Turkey is projected to have more precipitation in this season. There is a small belt of precipitation decrease over the upper Seyhan River region, where decrease becomes more evident in summer. In summer (JJA) most of Turkey experiences decreased rainfall in this model projection. In fall (SON), decreased precipitation over the Mediterranean region becomes dominant again with a northern wet and southern dry contrast.

Figure 3 shows the changes in evaporation. Generally evaporation increases in all seasons, but this field is distinct in a clear contrast between land and the oceans. There are large evaporation increases over the Mediterranean and the Black Sea in summer, fall and winter seasons, while in spring

evaporation increase over land is larger. Evaporation decreases are only projected over southern part of Turkey in summer and over eastern Mediterranean countries in spring and summer. Decreased evaporation in these regions may be related to soil moisture changes, but further investigation is needed.

Figure 4 shows the changes in surface runoff. Except for the Black Sea coastal regions in fall and winter where runoff increased, there are overall decreases in runoff over most regions of Turkey. Even in areas of increased precipitation, evaporation excess overcompensates and surface runoff has decreased. This is particularly true over the central Anatolia in spring, where precipitation increased but runoff decreased. Over the lower Seyhan River Basin, decrease in runoff is projected in winter but changes its sign in spring. On the other hand, opposite runoff changes are seen over the upper Seyhan River area. In summer, there is little change in surface runoff, although precipitation decreases over the southern Anatolia region. Cancellation between precipitation changes and evaporation changes resulted in little changes in runoff in this season. These smaller scale features such as changes over the ICCAP area need careful analysis.

3. Summary

Ten-year simulations are performed with the 20-km mesh global AGCM for the present and future conditions, respectively. Due to increased resolution, synoptic scale atmospheric circulations are very well simulated together with orographic precipitation features. Different changes in precipitation and runoff between the Seyhan River Basin and mountain areas are interesting and need further investigations.

These very high resolution model's results would be very useful for regional climate change assessment because the global model has no artificial boundaries that regional models must use. A limitation of time integration due to huge computational resource and non-existence of air-sea interaction are trade-offs.

We plan to store the monthly mean data for 117 selected variables and daily data for 5 variables (daily maximum surface air temperature, daily minimum surface air temperature, daily maximum surface wind speed, daily precipitation and daily maximum one-hour precipitation) for Turkey and the surrounding region for 10 year each for present and future for the use in the ICCAP project.

Acknowledgment

This result is based on a time-slice experiment performed by a Global Modeling Group (T.Matsuo, T.Aoki, A.Noda, S.Kusunoki, A.Kitoh, M.Hosaka, J.Yoshimura, S.Yukimoto, H.Yoshimura, T.Uchiyama, T.Yasuda, K.Shibata, M.Mikami, H.Ichizaki, H.Tsujino, Y.Takeuchi, T.Matsumura, H.Kitagawa, K.Katayama, M.Nakagawa, M.Kyouda, K.Yamada, M.Hirai, T.Hosomi, R.Sakai, S.Murai, M.Yamaguchi, T.Sakashita, A.Narui, T.Kadowaki, M.Kazumori, T.Ose, S.Maeda, C.Kobayashi, H.Kawai, K.Horiuchi, K.Ouchi, R.Mizuta, K.Miyamoto, H.Murakami, K.Fukuda) under the research project "Development of Super High Resolution Global and Regional Climate Models" funded by the Ministry of Education, Culture, Sports, Science and Technology (MEXT).

References

Aoki, T., A. Noda, M. Yoshizaki and Kyosei-4 Modeling Group, 2004: Development of Super High Resolution Global and Regional Climate Models on the Earth Simulator for the Projection of Global Warming. *Presented at First International CLIVAR Science Conference, June 21-25, 2004, Baltimore, Maryland, USA.*

IPCC, 2001: *Climate Change 2001: The Scientific Basis. Contribution of Working Group I to the Third Assessment Report of the Intergovernmental Panel on Climate Change.* Houghton, J.T. et al. (eds.), Cambridge University Press, 881pp.

Yukimoto, S., A. Noda, A. Kitoh, M. Sugi, Y. Kitamura, M. Hosaka, K. Shibata, S. Maeda and T. Uchiyama, 2001: The new Meteorological Research Institute coupled GCM (MRI-CGCM2). –Model climate and variability–. *Pap. Meteor. Geophys.*, **51**, 47-88.

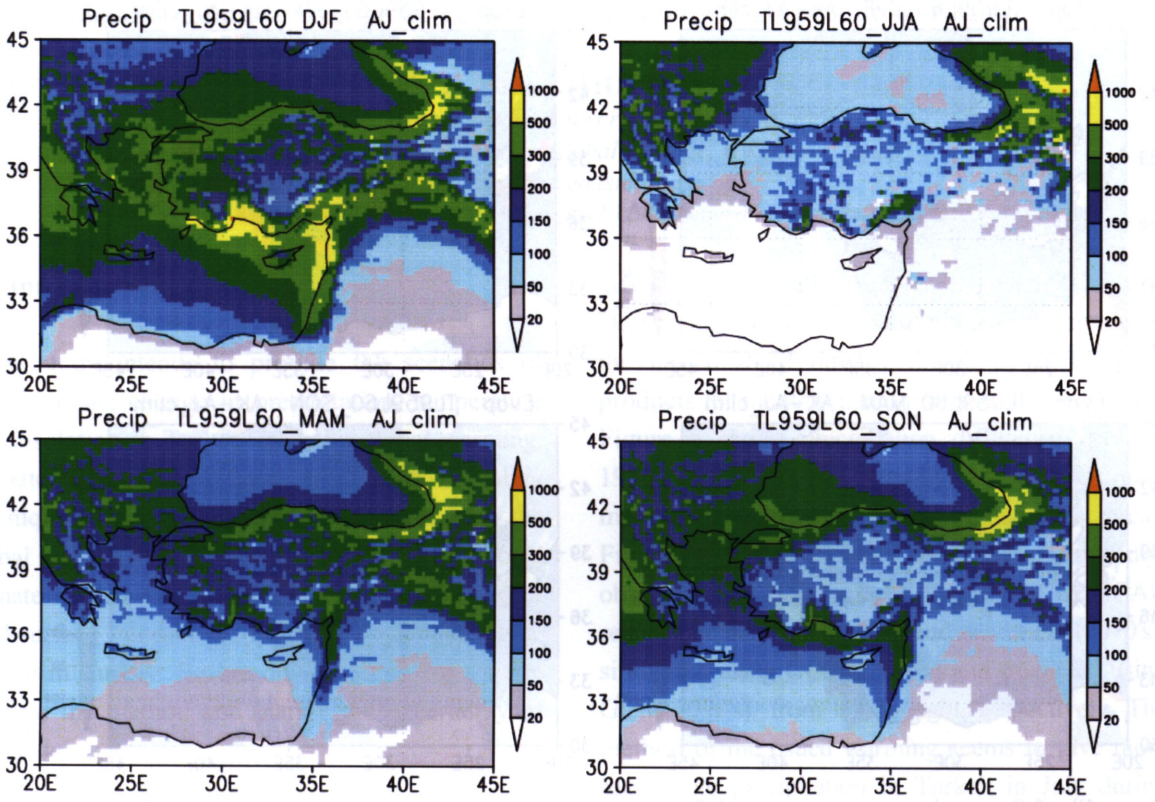

Fig. 1 Ten-year mean seasonal meanprecipitation in the TL959L60 control integration (P).

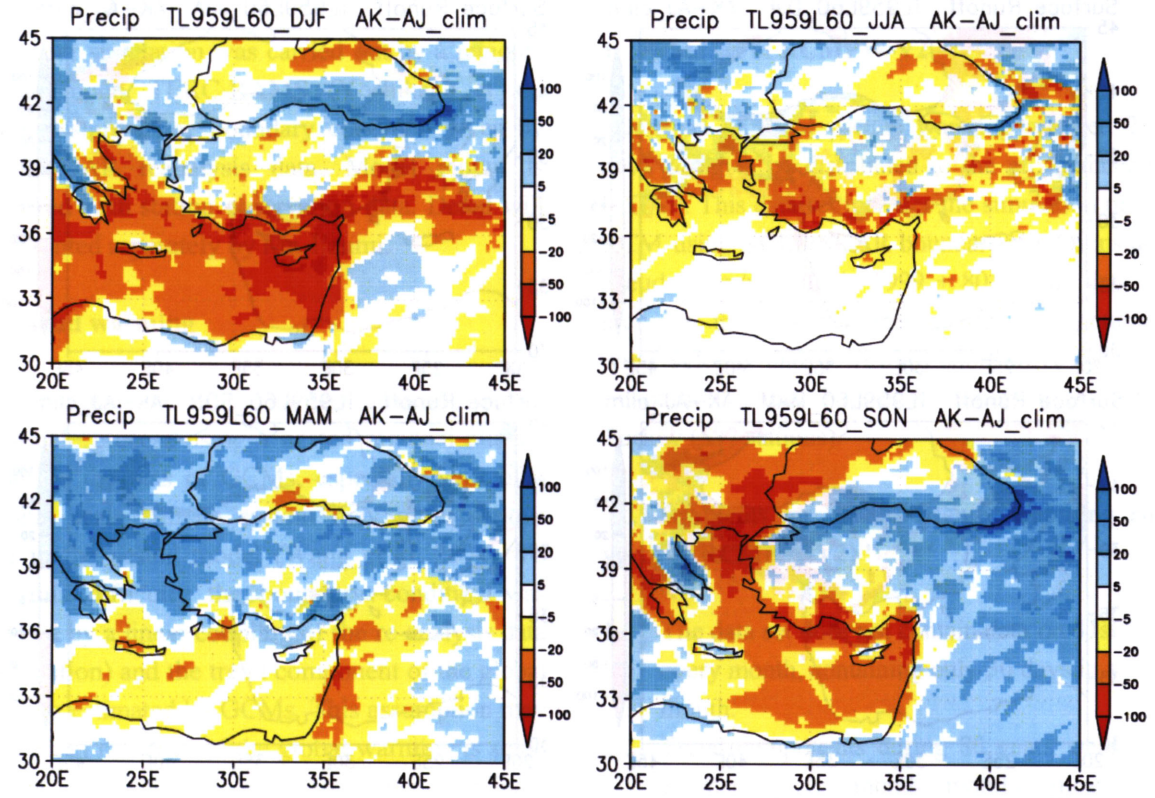

Fig. 2 Seasonal mean precipitation difference (future minus present) by the TL959L60 model.

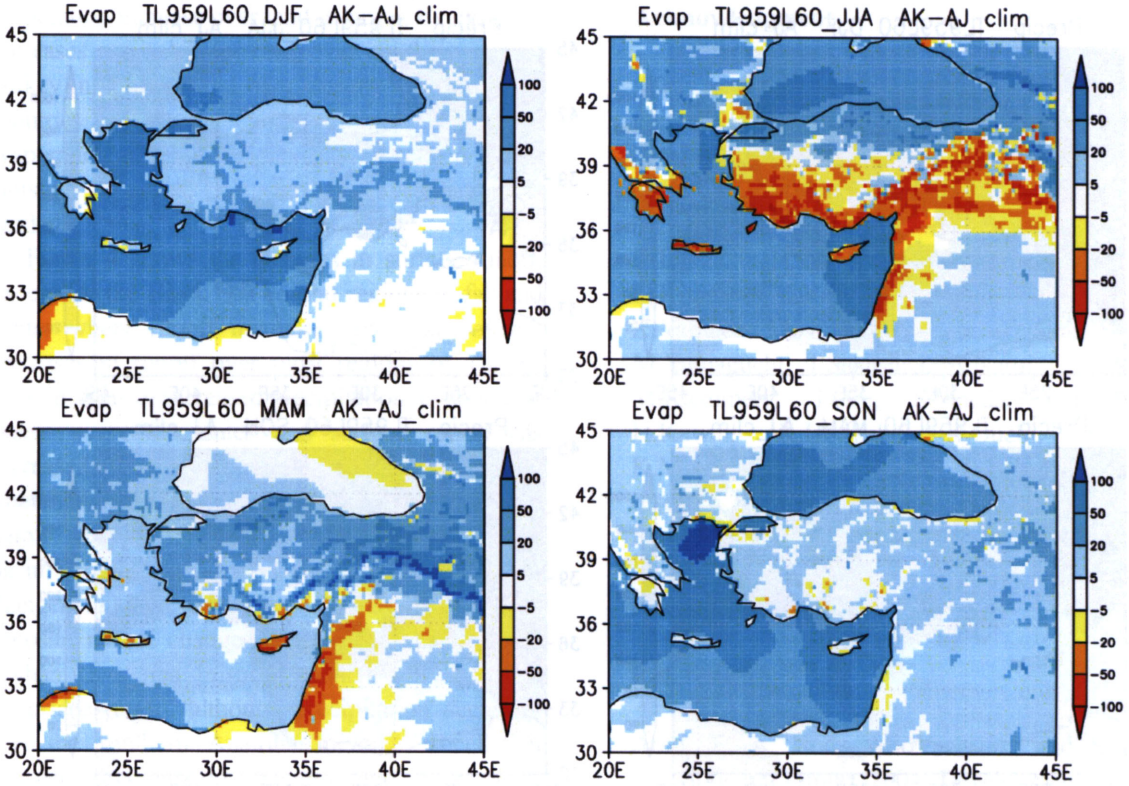

Fig. 3 Seasonal mean evaporation difference (future minus present) by the TL959L60 model.

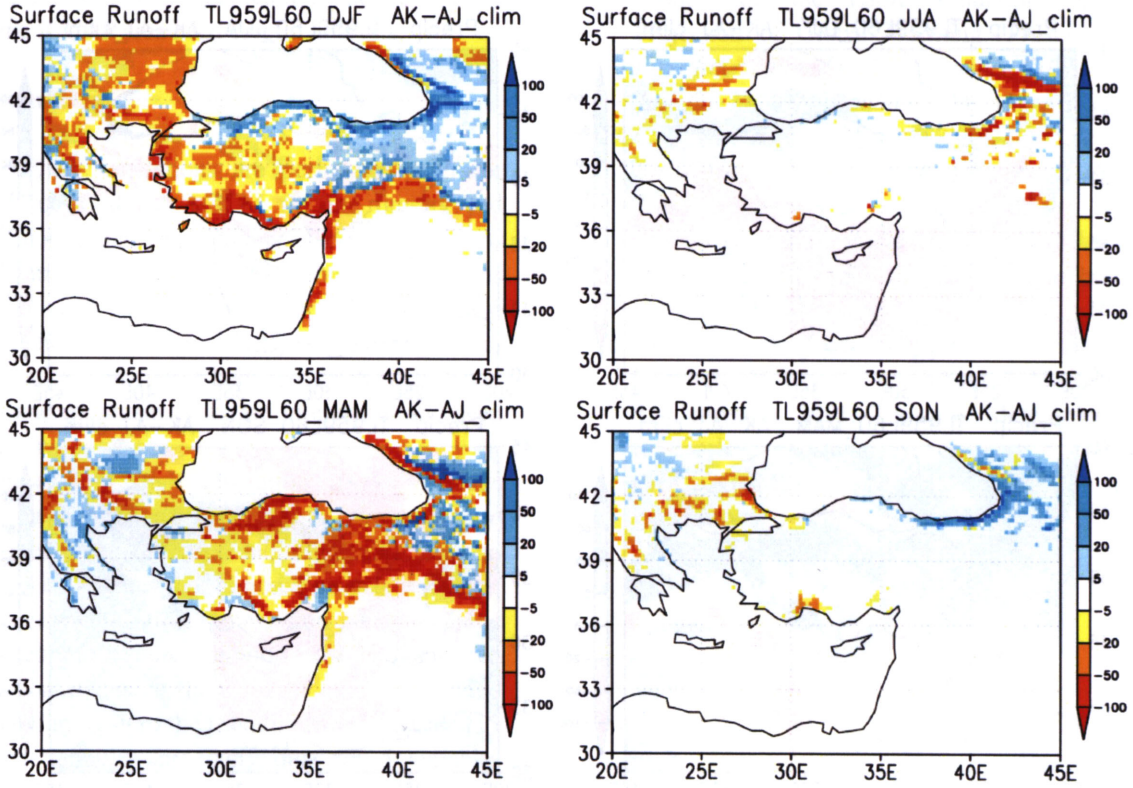

Fig. 4 Seasonal mean surface runoff difference (future minus present) by the TL959L60 model.